J. Fluid Mech. (1977), *vol.* 80, *part* 4, *pp.* 757–767
Printed in Great Britain

Cavitation in lubrication. Part 2. Analysis of wavy interfaces

By M. D. SAVAGE
School of Mathematics, University of Leeds, England

(Received 31 May 1976)

The steady and uniform flow of a viscous fluid past a uniform cavity in a geometry with small, yet arbitrary, film thickness is considered. A mathematical model for describing steady perturbations to such a flow is presented in which the perturbation to the cavity–fluid interface is represented by a small amplitude harmonic wave of wavenumber n. A linearized perturbation analysis then permits the formulation of a boundary-value problem involving the homogeneous Reynolds equation, the solution to which determines both n and the perturbed pressure field.

Numerical and approximate analytic solutions are determined for the cylinder–plane geometry in which fluid flows between a rotating cylinder and a Perspex block. Whilst these compare well with experimental data over the whole range

$$0{\cdot}1 < \eta U/T < 3,$$

closest agreement between theory and experiment is attained for small values of both $\eta U/T$ and n.

1. Introduction

A familiar feature in the flow (i) between counter-rotating rollers, (ii) in a cylinder–plane geometry or (iii) in a journal bearing is the presence of an air cavity. This arises either by ventilation or when dissolved air is expelled from the viscous lubricant once its pressure falls below saturation pressure.

Figure 1(*c*) of part 1 shows a cylinder–plane geometry designed so as to provide a variable minimum film thickness h_0 between a Perspex block and a variable-speed cylinder. The air cavity is formed downstream of the position of minimum film thickness and can be viewed from above directly through the Perspex block. Figures 1(*a*)–(*d*) (plate 1) and figure 2 (plate 2) show the transition from a straight cavity–fluid interface to a wavy interface to one of increasing wavenumber, obtained by maintaining a constant cylinder speed and gradually decreasing the minimum film thickness h_0. On examination the cavity–fluid interface appears to exhibit a harmonic waviness for small n, yet as n increases distortions arise, causing the interface eventually to rupture, in which case the air cavity is seen to consist of a series of adjacent air fingers separated by narrow columns of fluid (figure 2). In part 1 the transition of an interface from a straight line to waviness was considered and a criterion established. The aim of this investigation is to model the flow once perturbations have arisen and to determine those physical parameters upon which the wavenumber depends.

Previous work on this and related problems, by Floberg and Pearson in particular, provides much insight and offers two distinct lines of approach. Floberg (1957) sought a numerical solution for the pressure distribution in a cylinder–plane geometry in

which the film thickness was given by $h(x) = h_0(1 + x^2/2Rh_0)$, with R representing the radius of the cylinder and x measuring distance downstream of the point of minimum film thickness. In his model Floberg ignored surface tension and assumed that the air cavity spanned the full width of the gap between cylinder and block, thus forcing all the fluid into the narrow channels separating adjacent air fingers. Such an assumption is obviously invalid for small n (figures 1*a–d*) and consequently his analysis has relevance only in the large n regime. Together his numerical and experimental results (obtained using apparatus similar to that shown in figure 1(*c*) of part 1) confirmed a correlation between (i) the number of air fingers and the non-dimensional minimum fluid pressure, (ii) the number of air fingers and the location of the cavity boundary and (iii) the number of air fingers and the load capacity.

Pearson, in an earlier paper (1960), records evidence of phenomena similar to that investigated in this paper in a variety of contexts including the tin plate, the printing ink, the photographic and the paint industries. Pearson was concerned with the problem of 'spreading': the effect produced by moving a roller without rotation perpendicular to its axis over a flat surface covered with a viscous fluid. He sought an analytic solution on the basis that the air fingers arose owing to the presence of a secondary disturbance on the main flow. Mathematical difficulties, however, caused him to restrict his attention to the analysis of a spreader in the form of a wide-angled wedge. By introducing time-dependent perturbations proportional to $e^{st}\cos ny$, where t is time and y is distance along the axis of the spreader, he was able to obtain theoretical results which compared favourably with his experimental findings when the parameter $\eta U/T$ was not large by making the following assumption: that those wavenumbers which maximize s will dominate the early stages of the instability and will characterize the ultimate steady secondary flow. Also, in direct contrast to Floberg he assumed that the fluid which flows beneath the cavity when the interface is continuous (figures 1*a–d*) continues to do so when the interface ruptures (figure 2), none being diverted into the channels separating adjacent air fingers.

In the following section a mathematical model is developed which incorporates a linearized perturbation analysis in the manner of Pearson but in which the perturbations are steady, thus avoiding the use of a dubious assumption concerning the growth of small disturbances. Whereas Pearson was handicapped by not having a complete set of boundary conditions for determining explicitly the position of the cavity in the uniform two-dimensional flow, we shall use Coyne & Elrod's (1971) conditions as described in part 1. Consequently linearized theory gives rise to two boundary-value problems each involving the Reynolds equation and three boundary conditions. The first describes the uniform flow (pressure distribution and position of the cavity) whilst the second governs the perturbed flow, the solution to which yields the perturbed pressure field and the wavenumber n.

In § 3 the flow in a cylinder–plane geometry is considered and two methods of solution to the second boundary-value problem are examined. The Runge–Kutta procedure enables the determination of a numerical solution which suggests that if $\eta U/T$ is held constant the wavenumber should increase with increasing R/h_0. That this is indeed the case was established experimentally using several lubricants and covering the range $0{\cdot}1 < \eta U/T < 3$. Agreement between theory and experiment is particularly good for small n and small values of $\eta U/T$, which is to be expected since once n reaches a certain magnitude the assumption that the cavity interface can be represented by a

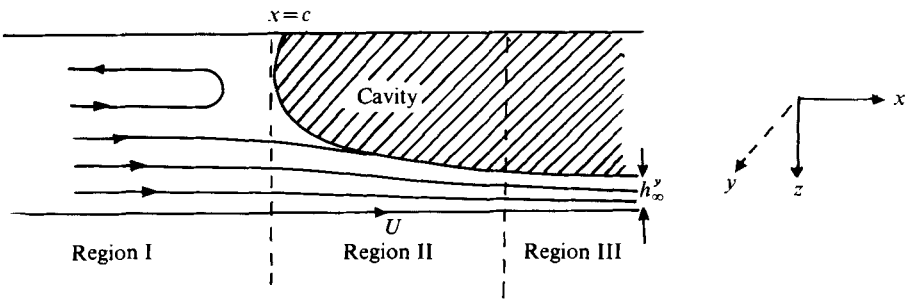

FIGURE 3. An x,z cross-section of the flow past the cavity showing part of (I) the lubrication region, (II) the transition region and (III) the region of uniform flow.

harmonic wave obviously fails whilst the results of Coyne & Elrod are suspect once $\eta U/T$ exceeds the order of unity.

Of special interest in this problem is the behaviour of n as R/h_0 is decreased ($\eta U/T$ remaining constant). Does n tend uniformly to zero at the critical value of R/h_0 given by the stability criterion discussed in part 1 or indeed at some other value of R/h_0? An analytic solution, obtained by suitably approximating the Reynolds equation, clearly demonstrates that (i) the stability criterion is too strong a condition for predicting the transition from a straight cavity–fluid interface to one represented by a harmonic wave, (ii) when waviness first arises it is characterized by a distinct non-zero wavenumber N^0, and (iii) on the graph of wavenumber against R/h_0, $(N^0, (R/h_0)^0)$ corresponds to a point of bifurcation from which emerge two branches such that at any R/h_0 above the minimum there exist two possible values of the wavenumber. Of the two branches it is the large n branch which is manifested in practice whilst theoretically it is possible to identify this solution as the one which incurs the least rate of energy dissipation.

2. Mathematical model

Figure 3 shows an x,z cross-section of the flow through a gap of arbitrary thickness $h(x)$ in the vicinity of the cavity whilst figure 2 (b) of part 1 provides an x,y cross-section of a cavity–fluid interface subject to a harmonic perturbation. In such a flow the pressure distribution $P(x,y)$ is given by the Reynolds equation once the usual assumptions of lubrication theory have been invoked;

$$\frac{\partial}{\partial x}\left(h^3\frac{\partial p}{\partial x}\right)+\frac{\partial}{\partial y}\left(h^3\frac{\partial p}{\partial y}\right)=6\eta U\frac{\partial h}{\partial x}. \tag{2.1}$$

If the pressure is specified as atmospheric (zero) at $x=-\infty$ and if $x=c$ is the position at which the cavity forms, then both c and the pressure $P^0(x)$ in a uniform flow subject to no perturbations are determined from the following boundary-value problem:

$$\frac{\partial}{\partial x}\left(h^3\frac{\partial p^0}{\partial x}\right)=6\eta U\frac{\partial h}{\partial x}, \tag{2.2}$$

$$p^0(-\infty)=0, \quad p^0(c)=-T/r, \tag{2.3),(2.4}$$

$$p_x^0(c)=\frac{\partial p^0}{\partial x}(c)=\frac{6\eta U}{h^2(c)}\left(1-2\frac{h_\infty}{h(c)}\right), \tag{2.5}$$

where $r = \beta h(c)$ is the radius of curvature of the cavity interface in the x, z plane, $h_\infty = \alpha h(c)$, and both α and β are functions of $\eta U/T$ only whose values have been computed by Coyne & Elrod (1971).

Once steady perturbations arise, if we assume them to vary harmonically with y and to be of magnitude ϵ ($\epsilon \ll c$) and wavenumber n then $x = c + \epsilon \sin ny$ becomes the new location of the cavity–fluid interface whilst the pressure distribution can be expressed as

$$P(x, y) = P^0(x) + \epsilon G(x) \sin ny. \tag{2.6}$$

The objective is now to determine both n and $G(x)$.

In the x, y plane, the velocity distribution (u, v) satisfying the boundary conditions $u = v = 0$ on $z = 0$ and $u = U$, $v = 0$ on $z = h(x)$ is given by

$$\left.\begin{aligned} u(x, y, z) &= \frac{p_x^0(z^2 - zh)}{2\eta} + U\frac{z}{h} + \frac{\epsilon G_x(z^2 - zh)}{2\eta} \sin ny, \\ v(x, y, z) &= \frac{\epsilon G(z^2 - zh)}{2\eta} n \cos ny. \end{aligned}\right\} \tag{2.7}$$

In addition the governing differential equation for $G(x)$ is found by substituting (2.6) into (2.1), as a result of which terms of order ϵ yield

$$G_{xx} + (3h_x/h) G_x - n^2 G = 0. \tag{2.8}$$

Again taking the pressure at infinity to be atmospheric gives $G(-\infty) = 0$ whilst at the cavity fluid and surface-tension pressures balance each other if we assume the cavity pressure also to be atmospheric. Hence

$$P(c + \epsilon \sin ny) + \epsilon G(c + \epsilon \sin ny) \sin ny = \frac{-T}{\beta h(c + \epsilon \sin ny)} + \epsilon T n^2 \sin ny,$$

the last term representing that contribution to surface-tension pressure arising from curvature in the x, y plane. Linearizing and equating terms of order ϵ yields the relationship

$$G(c) = Th_x(c)/\beta h^2(c) - P_x^0(c) + n^2 T. \tag{2.9}$$

A further condition on $G(x)$ is obtained via an equation of continuity. Figure 3 shows an x, z cross-section through any station y, in which fluid possessing velocity components in the x and y directions approaches the cavity in region I and subsequently passes through a transition region, region II, before emerging into region III in a uniform layer of thickness h_∞^y. Following Coyne & Elrod the transition region will be of order $h(c)$ in extent, so that gradients with respect to both x and z far exceed those with respect to y, i.e. $\partial/\partial x \gg \partial/\partial y$ and $\partial/\partial z \gg \partial/\partial y$. Consequently there will be no lateral diffusion in the transition region, the flow being essentially two-dimensional (in the x, z plane), and continuity of flow requires that

$$\int_0^{h(c + \epsilon \sin ny)} u(x, y, z)\, dz = Uh_\infty^y, \tag{2.10}$$

from which is derived the expression

$$P_x^0(x + \epsilon \sin ny) + \epsilon G_x(c + \epsilon \sin ny) \sin ny = \frac{6\eta U}{h^2(c + \epsilon \sin ny)} \left[1 - \frac{2h_\infty^y}{h(c + \epsilon \sin ny)}\right]. \tag{2.11}$$

At this stage it is convenient to employ an important result from the work of Coyne & Elrod, namely that when $\eta U/T$ is constant the ratio of the thickness of the uniform layer at infinity to the film thickness at the leading edge of the cavity is also constant; hence for all y

$$\frac{h_\infty^y}{h(c+\epsilon\sin ny)} = \frac{h_\infty}{h(c)} = \alpha. \tag{2.12}$$

Linearizing (2.11) and using (2.12) provides the required condition:

$$G_x(c) = -P_{xx}^0(c) - \frac{12\eta U h_x(c)}{h^3(c)}(1-2\alpha). \tag{2.13}$$

Eliminating $P_{xx}^0(c)$ via (2.2) and (2.5) and introducing the change of variables $x = (2Rh_0)^{\frac{1}{2}}X$ ($c = (2Rh_0)^{\frac{1}{2}}C$), $G(x) = (6\eta U/h^2(c))\,g(X)$, $n(2Rh_0)^{\frac{1}{2}} = N$ permits the formulation of the following boundary-value problem for $g(X)$ and N:

$$g_{XX} + (3h_X/h)\,g_X - N^2 g = 0, \quad -\infty < X \leqslant C, \tag{2.14}$$

$$g(-\infty) = 0, \tag{2.15}$$

$$g(C) = -(1-2\alpha) + \frac{T}{6\eta U\beta}\frac{h_X(c)}{(2Rh_0)^{\frac{1}{2}}} + \frac{T}{12\eta U}\frac{N^2h^2}{Rh_0}, \tag{2.16}$$

$$g_X(C) = (-2h_X/h)\,\alpha. \tag{2.17}$$

Before solving (2.14)–(2.17) for a particular geometry, certain deductions are possible; in particular $g(C)$ must be less than zero for any solution to exist. This result is deduced by way of the following argument. Equation (2.14) can be used to infer that $g(X)$ has no maxima or minima over the range $-\infty < X \leqslant C$. Hence (2.15) implies that $g(X)$ tends monotonically to zero at infinity from its specified value at $X = C$ and consequently both $g(C)$ and $g_X(C)$ must have the same sign. Consequently perturbations arise only when $g(C) < 0$. Conversely there is no solution (and so no perturbation) when $g(C) \geqslant 0$, i.e.

$$\frac{T}{6\eta U\beta}\frac{h_X}{(2Rh_0)^{\frac{1}{2}}} \geqslant 1-2\alpha, \tag{2.18}$$

which is precisely the criterion established in part 1. Whilst this criterion guarantees the stability of a uniform flow (and a uniform cavity–fluid interface) it does not follow that when this criterion fails harmonic perturbations will immediately arise. In fact

$$\frac{T}{6\eta U\beta}\frac{h_X}{(2Rh_0)^{\frac{1}{2}}} < 1-2\alpha$$

is a necessary but not a sufficient condition for the existence of a solution to (2.14)–(2.17), a fact which will become clear in the following section.

3. Method of solution

Turning our attention to the cylinder–plane geometry, in which the film thickness is given by $h(X) = h_0(1+X^2)$, the preceding boundary-value problem becomes

$$g_{XX} + \frac{6X}{1+X^2}g_X - N^2 g = 0, \quad -\infty < X \leqslant C, \tag{3.1}$$

$$g(-\infty) = 0, \tag{3.2}$$

$$g(C) = -(1-2\alpha) + \frac{T}{6\eta U\beta}\left(\frac{2h_0}{R}\right)^{\frac{1}{2}} C + \frac{T}{12\eta U}\left(\frac{h_0}{R}\right) N^2(1+C^2)^2, \tag{3.3}$$

$$g_X(C) = -\frac{4C}{1+C^2}\alpha. \tag{3.4}$$

This is complete once the substitution $C = \tan\gamma^C$ is made and (2.2)–(2.5) are solved to obtain a relationship between γ^C, R/h_0 and $\eta U/T$:

$$-\frac{T}{12\eta U\beta}\left(\frac{2h_0}{R}\right)^{\frac{1}{2}} \cos^2\gamma^C = \left(\frac{\gamma^C}{2} + \frac{\pi}{4} + \frac{\sin 2\gamma^C}{4}\right) - \frac{2\alpha}{\cos^2\gamma^C}\left[\left(\frac{3\gamma^C}{8} + \frac{3\pi}{16} + \frac{\sin 2\gamma^C}{4} + \frac{\sin 4\gamma^C}{32}\right)\right]. \tag{3.5}$$

It is apparent that N depends only upon the two independent parameters R/h_0 and $\eta U/T$ and can be determined numerically using the Runge–Kutta procedure. To begin with, values are assigned to R/h_0 and $\eta U/T$ and subsequently γ^C is determined from (3.5). A 'suitable' guess is then made for N, which enables (3.1) to be solved in conjunction with boundary conditions (3.3) and (3.4), as a result of which a value of $g(-B)$ is obtained, where B is a suitably chosen, large and positive real number. N is now varied until $g(-B)$ becomes 'sufficiently close' to zero and eventually, after some labour, a value of N is obtained for each pair of parameter values $(\eta U/T, R/h_0)$. It is relevant to add that experimental results provided the basis for making the initial choice of N and at no time did we suspect or indeed discover (numerically) the existence of more than one solution for N for each parameter pair $(\eta U/T, R/h_0)$. Experimental and numerical results are contrasted in figures 4(*a*)–(*c*), which also include results obtained via an approximate analytic method, which will now be considered.

4. An approximate analytic solution

The determination of an exact analytic solution to (3.1) is hindered by the coefficient of g_X, namely $3h_X/h$, which is associated with the geometry. This coefficient also appears in (2.2), where it is crucial in determining the location of the cavity. Its significance in (3.1) is much less crucial since here the first two terms govern the decay of the perturbations which are generated at the interface. Intuition suggests and experiment confirms that the perturbations do decay rapidly over a distance of the order of $(Rh_0)^{\frac{1}{2}}$ such that at $x = 0$, the position of minimum film thickness, there is virtually no trace of the perturbed flow. This being the case it is not unreasonable to approximate h_X/h by its value at the cavity and thus derive the solution

$$g(X) = g(C)\, e^{w(X-C)} \tag{4.1}$$

to (3.1), which also satisfies (3.2) and (3.3) and in which

$$w = -k + [k^2 + N^2]^{\frac{1}{2}}, \quad \text{where} \quad k = 3C/(1+C^2). \tag{4.2}$$

Finally condition (3.4) yields the relationship

$$-\frac{4C}{1+C^2}\alpha = w\left[-(1-2\alpha) + \frac{T}{6\eta U\beta}\left(\frac{2h_0}{R}\right)^{\frac{1}{2}} C + \frac{T}{12\eta U}\left(\frac{h_0}{R}\right) N^2(1+C^2)^2\right], \tag{4.3}$$

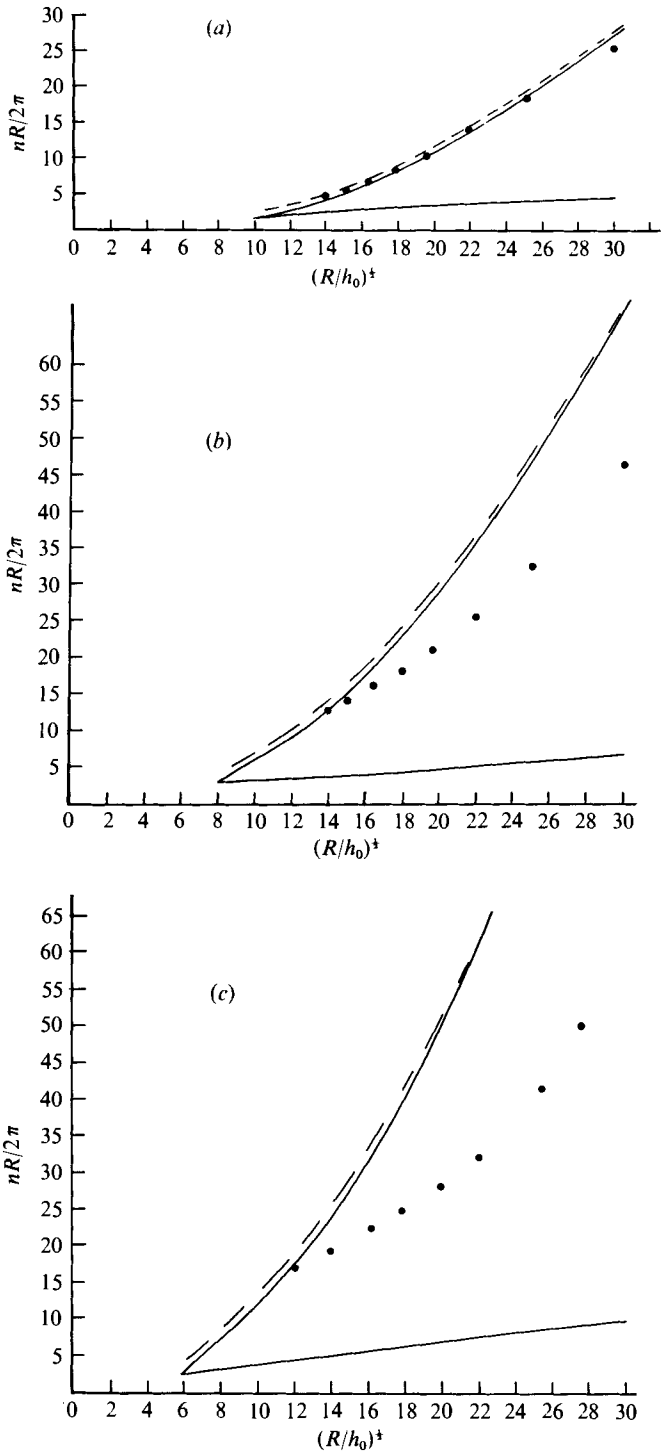

FIGURE 4. The number of waves in a width R against $(R/h_0)^{\frac{1}{2}}$ for (*a*) $\eta U/T = 0{\cdot}2$, (*b*) $\eta U/T = 0{\cdot}6$ and (*c*) $\eta U/T = 1{\cdot}4$. ●, determined experimentally; – – –, determined numerically; ——, determined analytically.

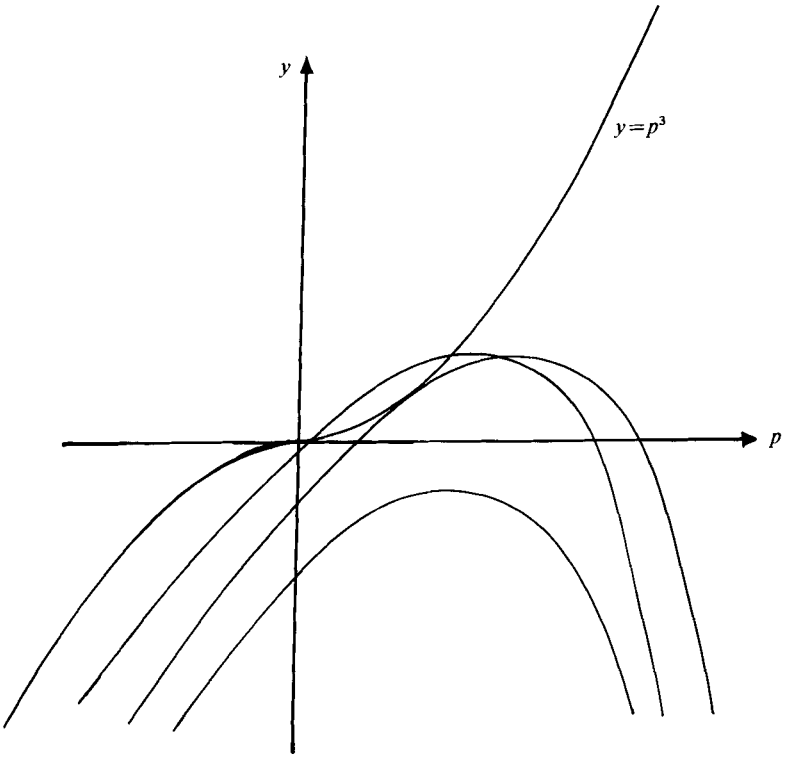

FIGURE 5. Graph of $y = p^3$ superimposed on $y = (a/b)\,p - 2kp^2 - d/b$ for three distinct sets of values of the coefficients $(a/b, -2k, -d/b)$ corresponding to three values of R/h_0 with $\eta U/T$ held constant.

and writing

$$a = (1-2\alpha) - \frac{T}{6\eta U\beta}\left(\frac{2h_0}{R}\right)^{\frac{1}{2}} C,$$

$$b = \frac{T}{12\eta U}\left(\frac{h_0}{R}\right)(1+C^2)^2, \quad d = \frac{4C\alpha}{1+C^2}$$

transforms (4.3) into

$$(k^2+N^2)^{\frac{1}{2}} = d/(a-bN^2) + k. \tag{4.4}$$

This can then be reduced to a cubic equation via the substitution $p = d/(a-bN^2)$:

$$p^3 + 2kp^2 - (a/b)\,p + d/b = 0. \tag{4.5}$$

As stated earlier, a necessary condition for the existence of a solution to (3.1)–(3.4) is $g(C) < 0$, i.e. $a - bN^2 > 0$, and since $d > 0$ such solutions correspond to positive real roots of (4.5). That this equation may exhibit two distinct, one or no positive real roots is readily seen from figure 5, in which $\eta U/T$ is held constant and the graph of $y = p^3$ is superimposed on those of $y = (a/b)\,p - 2kp^2 - d/b$ for three distinct values of R/h_0. The three parabolas intersect the cubic at respectively no, one and two points for which $p > 0$ and therefore correspond physically to (i) uniform flow, (ii) perturbed flow with a unique wavenumber and (iii) perturbed flow with two theoretically possible wavy modes.

Specifying R/h_0 and $\eta U/T$ and solving (4.5) for positive real p (when such solutions exist) enables the corresponding wavenumber(s) to be obtained and the results are displayed in figures 4(*a*)–(*c*).

5. Discussion of results

Figures 4 (*a*), (*b*) and (*c*) show the variation of $nR/2\pi$, the number of waves in a width equal to the cylinder radius, against $(R/h_0)^{\frac{1}{2}}$ for $\eta U/T = 0{\cdot}2$, $0{\cdot}6$ and $1{\cdot}4$ as determined experimentally and calculated both numerically and analytically. These curves clearly demonstrate that, for a given $\eta U/T$, (*a*) there is a critical value of R/h_0, say $(R/h_0)^0$, below which the basic two-dimensional flow is stable to harmonic perturbations, (*b*) this critical point is a point of bifurcation from which emerge two branches as (R/h_0) is increased and (*c*) experimental results confirm that it is the upper (large n) branch which is seen in practice.

The bifurcation point corresponds to (4.5) having two equal and positive roots, i.e. when the graph of $y = p^3$ just touches that of $y = (a/b)\,p - 2kp^2 - d/b$, at p^0 say. It is easily shown that this arises when

$$p^0 = \frac{3d}{2a}, \quad \tfrac{27}{4}bd^2 = a^3, \quad (nR)^2 = \frac{9}{6b}\left(\frac{R}{h_0}\right)^0, \quad N^0 = \left(\frac{3}{b}\right)^{\frac{1}{2}}, \tag{5.1}$$

the last expression giving that value of the wavenumber which characterizes the first perturbations to appear.

In this problem, as in certain others which exhibit bifurcation, the phenomenon of non-uniqueness can be considered in the light of an appropriate variational principle. Indeed, it is possible to identify the physical solution (for the disturbance) as the one which incurs the least rate of energy dissipation, as follows.

The Reynolds equation for the perturbation pressure $\bar{p}(X, y) = \epsilon G(X) \sin ny$ is

$$\frac{\partial}{\partial X}(h^3\bar{p}_X) + \frac{\partial}{\partial y}(h^3\bar{p}_y) = 0, \tag{5.2}$$

where the subscripts X and y indicate differentiation with respect to X and y respectively. This equation has a Lagrangian given by $L = h^3(\bar{p}_X^2 + \bar{p}_y^2)$ and may therefore be derived from the following variational principle:

$$\delta \iint_R h^3(\bar{p}_X^2 + \bar{p}_y^2)\,dX\,dy = 0, \tag{5.3}$$

where R is that domain of the X, y plane over which the disturbance is present.

Recall that any solution of (5.2) for $\bar{p}(X, y)$ is one which makes the integral appearing in (5.3) stationary. Then our current objective is to relate this integral to the solution seen in practice, i.e. the large n branch in figures 4 (*a*)–(*c*). However, owing to the periodicity in y we shall restrict our attention to the region

$$\bar{R} = \{-\infty < X \leqslant C,\ 0 \leqslant y \leqslant 2\pi/n\}$$

and consider the integral

$$\begin{aligned} I &\equiv \left(\frac{12\eta n}{\pi}\right) \int_{-\infty}^{C} \int_0^{2\pi/n} h^3(\bar{p}_X^2 + \bar{p}_y^2)\,dX\,dy \\ &= 12\eta\epsilon^2 \int_{-\infty}^{C} h^3(G_X^2 + n^2G^2)\,dX. \end{aligned} \tag{5.4}$$

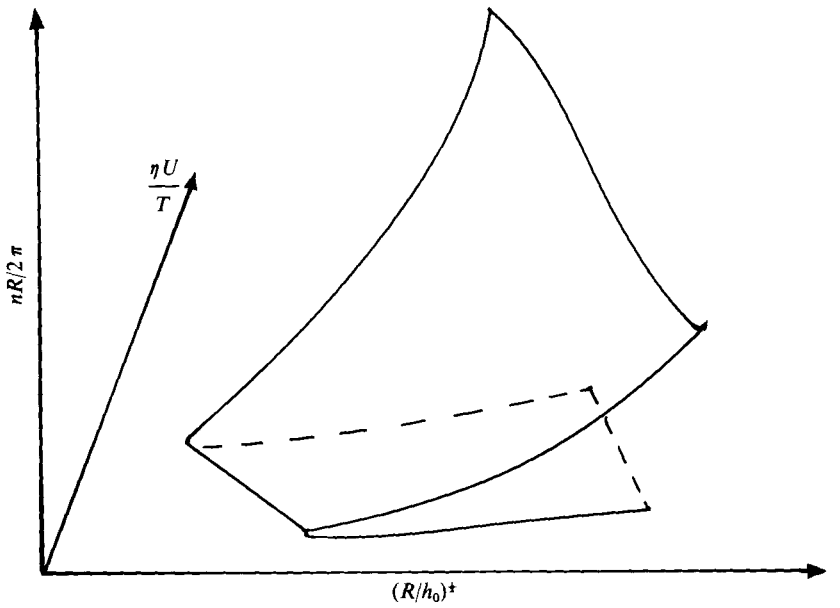

FIGURE 6. A plot of $nR/2\pi$ against the parameters $\eta U/T$ and $(R/h_0)^{\frac{1}{2}}$ producing an equilibrium surface with an elementary fold catastrophe.

If, in addition, we calculate the rate of energy dissipation $\bar{D}$ in a volume of fluid lying above the region $\bar{R}$ of the X, y plane (and include only derivatives with respect to z) we find that

$$\bar{D} = \int_{-\infty}^{C} \int_{0}^{2\pi/n} \int_{0}^{h(x)} \eta \left[\left(\frac{\partial u}{\partial z} \right)^2 + \left(\frac{\partial v}{\partial z} \right)^2 \right] dX\, dy\, dz, \tag{5.5}$$

where u and v are velocity components given by (2.7).

Hence the rate of energy dissipation D per unit width is given by $D = \bar{D}(2\pi/n)^{-1}$, which will include terms of order zero, order ϵ and order ϵ^2. The terms of zero order do not involve n, those of order ϵ disappear when the integration over y is performed whilst terms of order ϵ^2 combine to produce the integral I given by (5.4), which via the relation $(h^3 G_X)_X = n^2 h^2 G$ can be expressed in the form

$$I = 12\eta\epsilon^2 \int_{-\infty}^{C} [(h^3 G_X) G_X + (h^3 G_X)_X G]\, dx.$$

Thus

$$\begin{aligned} I &= 12\eta\epsilon^2 [h^3 G_X G]_{-\infty}^{C} \\ &= 12\eta\epsilon^2 h^3(C)\, G_X(C)\, G(C). \end{aligned} \tag{5.6}$$

In (5.6) both $h(C)$ and $G_X(C)$ are independent of n whilst $G(C) = -a + bN^2 < 0$ and therefore the magnitude of I decreases with increasing n. Hence it follows that the physical solution (the large n branch of figures 4 (*a*)–(*c*)) is the one which minimizes the function $I(n)$ and hence one which incurs the least rate of energy dissipation.

Referring once again to figures 4 (*a*)–(*c*), it is clear that there exists good agreement between theory and experiment during the early stages of instability, when n is small, but as n increases an overestimate of n is predicted and the divergence grows. Such a disparity arises since the twin assumptions of small amplitude ($\epsilon \ll c$) and the presence

of a harmonic wave on the interface begin to fail (figure 1*d*); and subsequently become invalid for larger n as shown in figure 2.

As catastrophe theory is currently in vogue, it is considered appropriate to present the results in the context of this theory, for which the behaviour variable n is plotted as a function of the two independent parameters $\eta U/T$ and R/h_0, thus giving rise to the equilibrium surface shown in figure 6. Such a surface corresponds to a fold catastrophe, which is the simplest of the elementary catastrophes described by Bröcker (1975).

Finally, appreciation is extended to Professor T. G. Cowling, who suggested a possible link between the physical solution and the rate of energy dissipation.

REFERENCES

Bröcker, T. H. 1975 *L.M.S. Lecture Note Series*, no. 17 (trans. L. Lander). Cambridge University Press.

Coyne, J. C. & Elrod, H. G. 1971 *A.S.M.E. Paper* no. 70 – Lub. 3.

Floberg, L. 1957 *Trans. Chalmers Univ. Tech.* no. 189.

Pearson, J. R. A. 1960 *J. Fluid Mech.* **7**, 481.

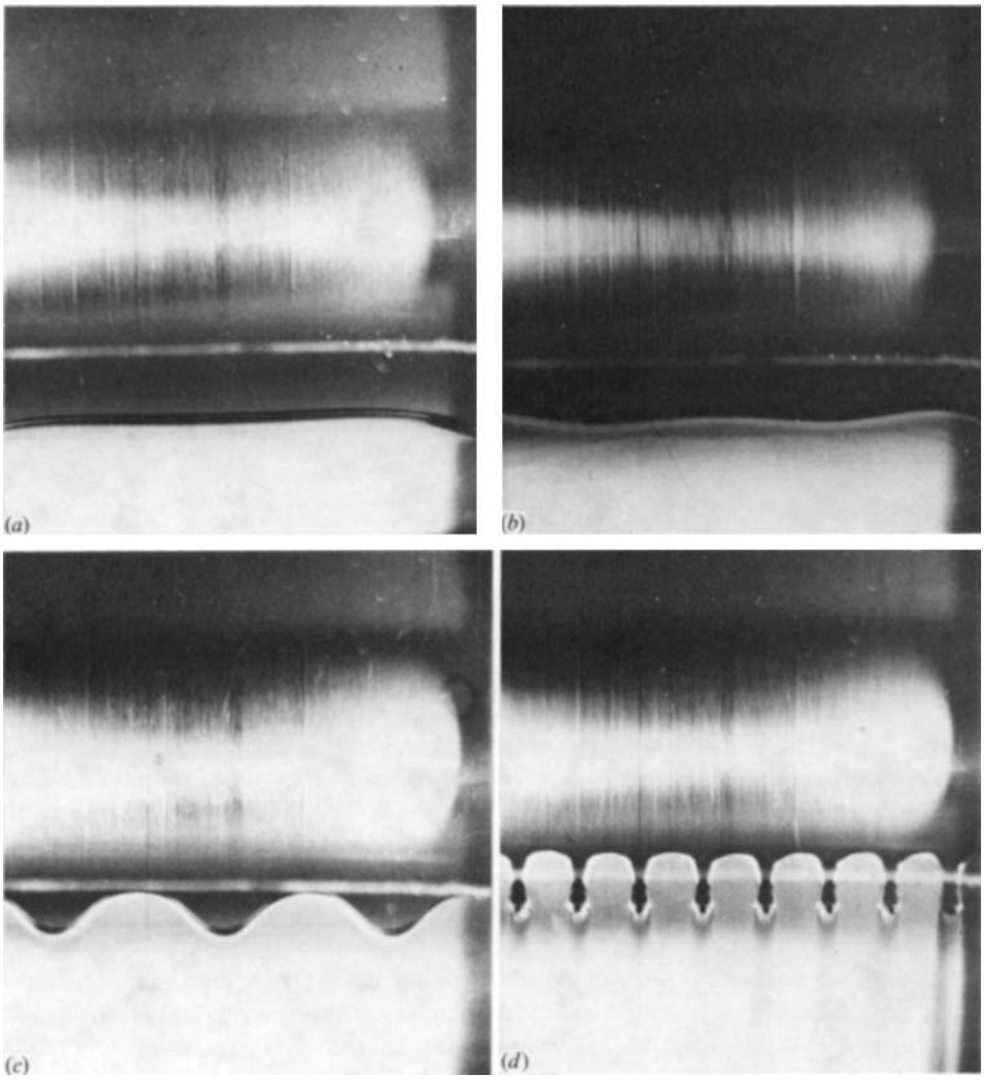

FIGURE 1. The transition from a straight cavity–fluid interface to a wavy interface.

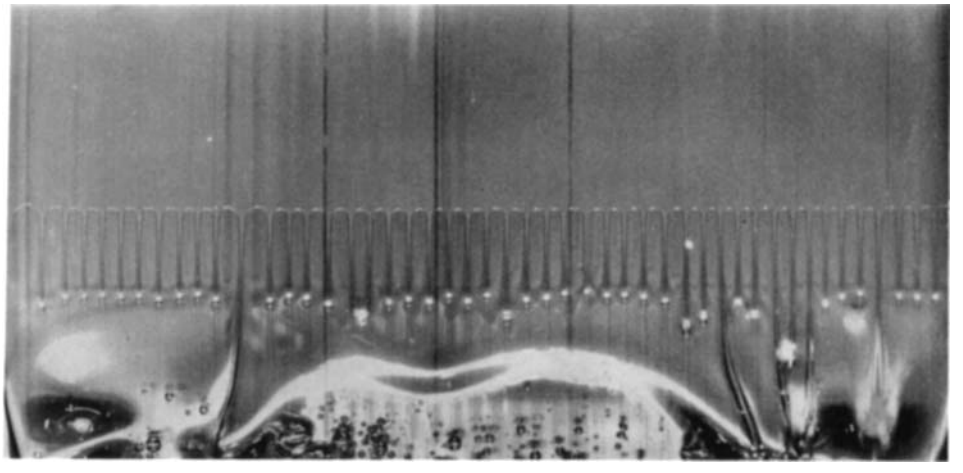

FIGURE 2. The large wavenumber regime, in which the interface consists of a series of adjacent air fingers.